Supplemental information

Histone Methyltransferase KMT2D Promotes Castration-Resistant Prostate Cancer Progression by Reactivating AR through FOXA1

Mayao Luo[1, 2, 3#], Chenwei Wu[2#], Manli Zhou[2], Yifan Zhang[1], Yadong Li[2], Yuanpeng Liao[1], Xin Huang[3], Chuance Du[3], Shidong Lv[1*], Qiang Wei[1, 2, 3*]*

[1]Department of Urology, Guangdong Cardiovascular Institute, Guangdong Provincial People's Hospital, Guangdong Academy of Medical Sciences, Southern Medical University, Guangzhou, Guangdong, 510080, China

[2]Department of Urology, Nanfang Hospital, Southern Medical University, Guangzhou, Guangdong, 510515, China

[3]Department of Urology, Ganzhou Hospital-Nanfang Hospital, Southern Medical University, Ganzhou, Jiangxi, 341000, China

Supplementary Figure 2

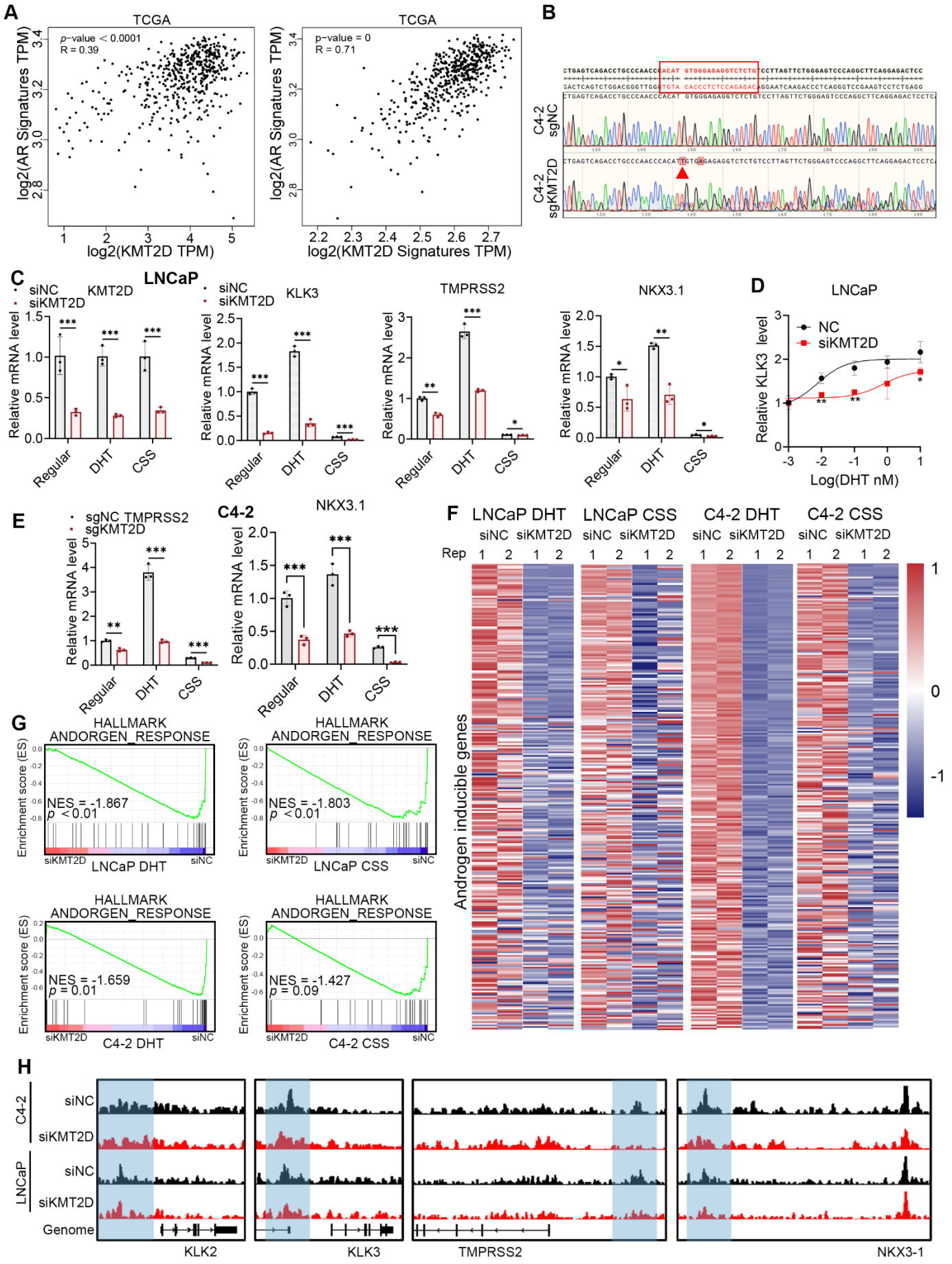

Supplementary Figure 2. KMT2D regulates AR signaling and target gene expression in prostate cancer cells, Related to Figure 2. (A) Positive correlations between KMT2D expression and AR signature scores (left), and between KMT2D signature and AR signature (right) in TCGA-PRAD cohort. Pearson correlation coefficients (R) and P values are shown. (B) Sanger sequencing chromatograms confirming CRISPR-mediated KMT2D knockout in C4-2 cells; red arrow indicates sgRNA target site. (C) qRT-PCR of KMT2D and AR target genes (KLK3, TMPRSS2, NKX3-1) mRNA levels in LNCaP cells after siRNA-mediated KMT2D knockdown under regular, DHT, or CSS conditions. (D) Dose-dependent reduction of KLK3 mRNA in LNCaP cells treated with increasing DHT concentrations following KMT2D silencing. (E) qRT-PCR quantification of TMPRSS2 and NKX3-1 mRNA levels in C4-2 cells with sgRNA-mediated KMT2D knockout under various culture conditions. (F) Heatmaps of androgen-responsive gene expression in LNCaP and C4-2 cells treated with siNC or siKMT2D under DHT or CSS conditions. (G) GSEA plots displaying negative enrichment of hallmark androgen response gene sets in siKMT2D-treated cells. (H) Genome browser snapshots showing decreased AR ChIP-seq signal at canonical AR target loci (KLK2, KLK3, TMPRSS2, NKX3-1) after KMT2D knockdown. Blue boxes indicate AR binding regions.

Supplementary Figure 4

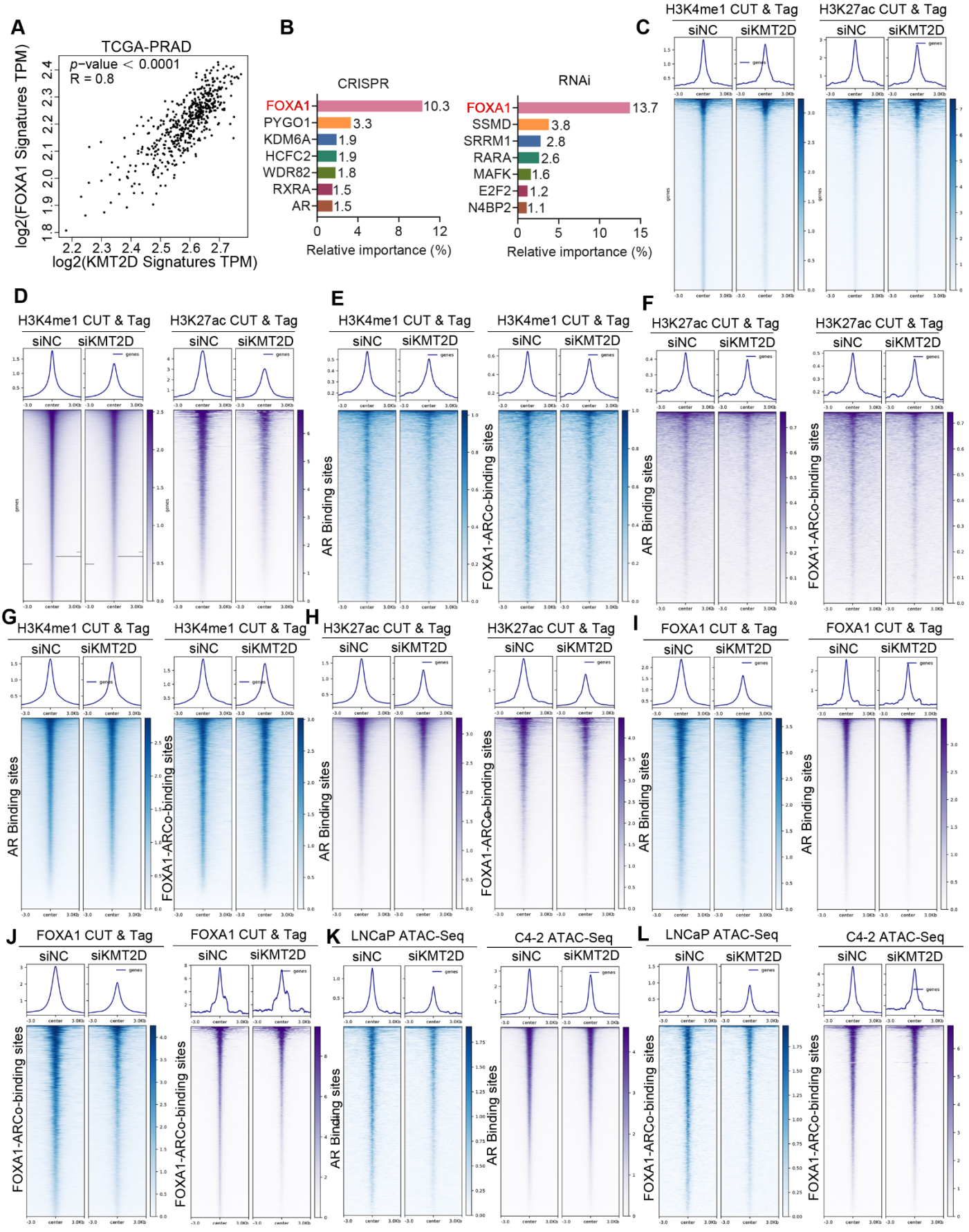

Supplementary Figure 4. KMT2D modulates chromatin accessibility and facilitates FOXA1-mediated AR target gene regulation, Related to Figure 4. (A) Positive correlation between KMT2D and FOXA1 signature expression in TCGA-PRAD cohort (Pearson R = 0.8, P < 0.0001).(B) Transcription factor relative importance scores from DepMap CRISPR (left) and RNAi (right) screens, highlighting FOXA1 as the top candidate.(C, D) CUT&Tag average profiles and heatmaps of H3K4me1 and H3K27ac signals in LNCaP (C) and C4-2 (D) cells treated with siNC or siKMT2D.(E, F) CUT&Tag average profiles and heatmaps of H3K4me1 and H3K27ac signals at AR binding sites and FOXA1-AR co-binding sites in LNCaP cells ± KMT2D knockdown.(G, H) CUT&Tag average profiles and heatmaps of H3K4me1 and H3K27ac signals at AR binding sites and FOXA1-AR co-binding sites in C4-2 cells ± KMT2D knockdown.(I, J) CUT&Tag average profiles and heatmaps of FOXA1 binding in LNCaP (I) and C4-2 (J) cells following siNC or siKMT2D treatment.(K, L) ATAC-seq average profiles and heatmaps showing chromatin accessibility at AR binding sites and FOXA1-AR co-binding sites in LNCaP (K) and C4-2 (L) cells with or without KMT2D knockdown.

Supplementary Figure 5

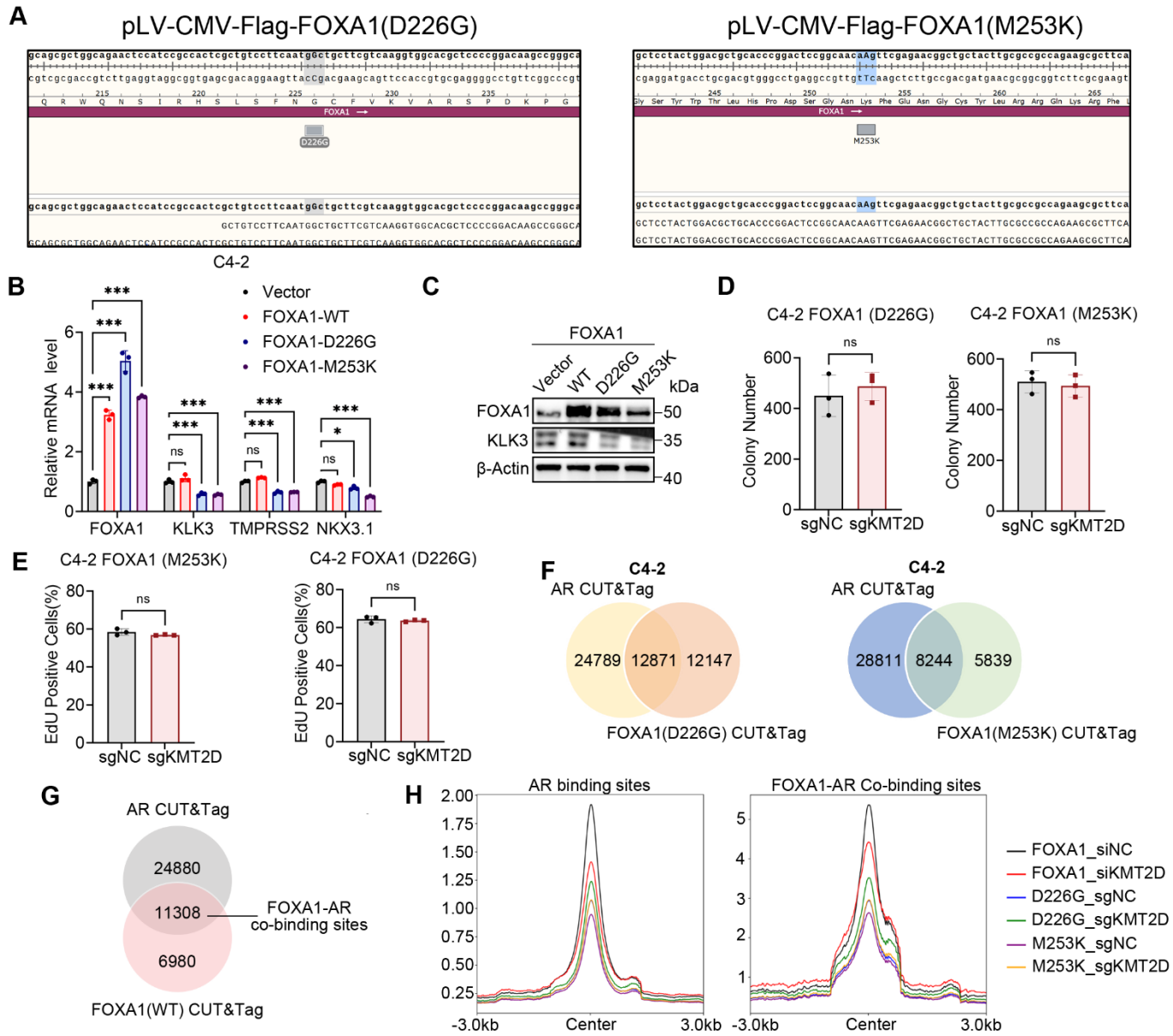

Supplementary Figure 5. FOXA1 missense mutations impair KMT2D-mediated regulation of AR signaling and prostate cancer cell proliferation, Related to Figure 5. (A) Schematic representation of FOXA1 missense mutations D226G and M253K located in the forkhead DNA-binding (FKHD) domain. (B) qRT-PCR analysis of FOXA1 and AR target genes (KLK3, TMPRSS2, NKX3-1) mRNA levels in C4-2 cells stably expressing wild-type (WT) or mutant FOXA1 (D226G, M253K). (C) Western blot showing FOXA1 and KLK3 protein expression in C4-2 cells expressing FOXA1 WT or mutants. β-Actin served as loading control. (D) Colony formation assays indicating that KMT2D knockout (sgKMT2D) fails to suppress proliferation in C4-2 cells expressing FOXA1 D226G or M253K mutants compared to control (sgNC). (E) EdU incorporation assays showing no significant change in proliferation upon KMT2D depletion in mutant FOXA1-expressing C4-2 cells. (F) Venn diagrams depicting overlap of AR CUT&Tag peaks with FOXA1 D226G (left) and M253K (right) CUT&Tag peaks in C4-2 cells. (G) Venn diagram showing overlap

between AR and wild-type FOXA1 CUT&Tag binding sites, highlighting FOXA1-AR co-binding regions. (H) CUT&Tag average profiles illustrating AR binding sites (left) and FOXA1-AR co-binding sites (right) in C4-2 cells expressing wild-type or mutant FOXA1 with or without KMT2D knockdown. FOXA1 mutants maintain AR and FOXA1 occupancy despite KMT2D depletion. Data represent mean ± SD; *P < 0.05, ***P < 0.001; ns, not significant.

Supplementary Figure 6

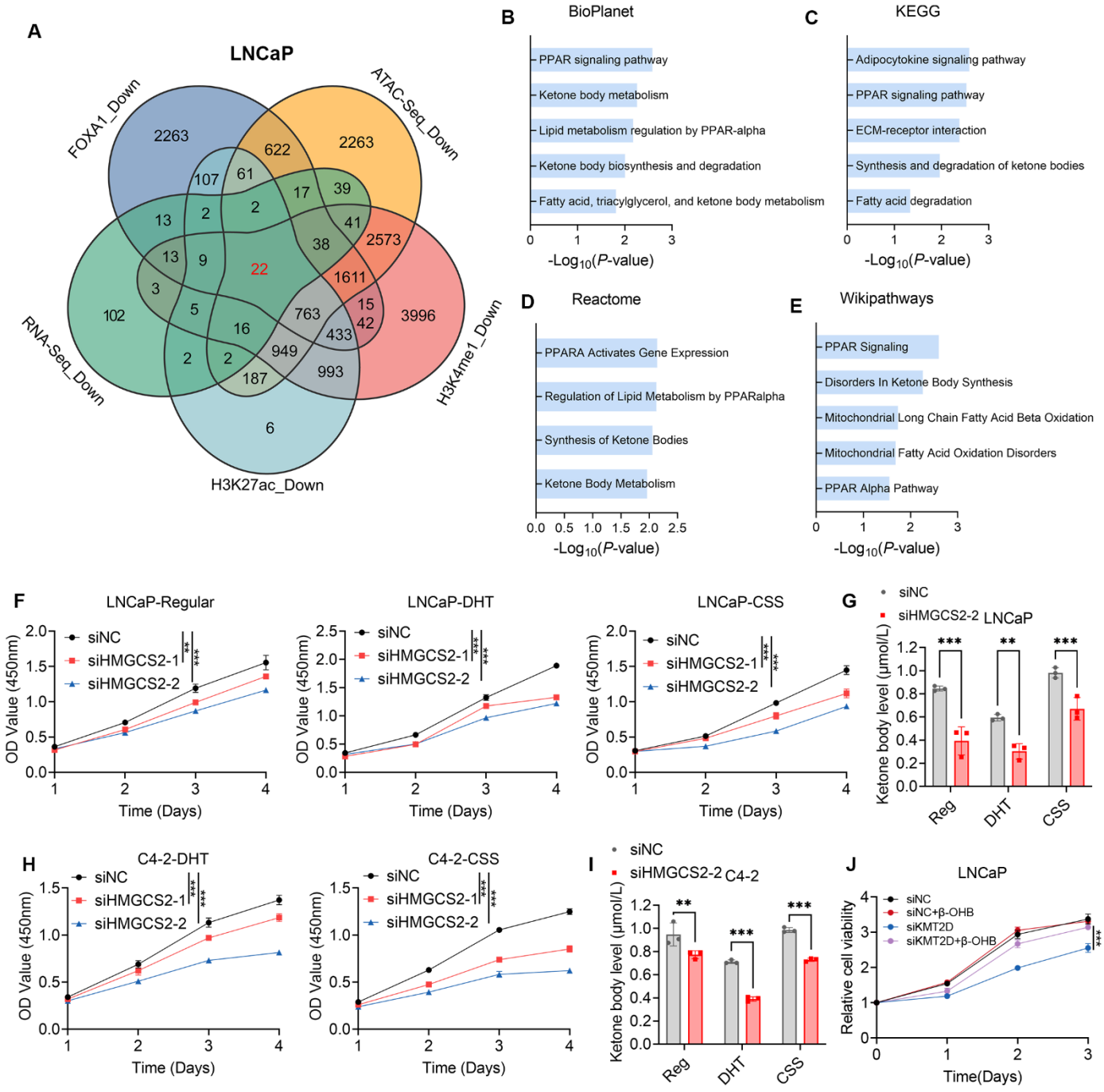

Supplementary Figure 6. HMGCS2 Downregulation Impairs Ketone Body Metabolism and Proliferation in Prostate Cancer Cells, Related to Figure 6. (A) Venn diagram showing the overlap of downregulated genes in LNCaP cells based on RNA-seq, ATAC-seq, H3K27ac ChIP-seq, and FOXA1 ChIP-seq datasets. A total of 22 overlapping genes were identified. (B-E) Pathway enrichment analysis of the overlapping genes using BioPlanet (B), KEGG (C), Reactome (D), and Wikipathways (E) databases. Prominent pathways include PPAR signaling, ketone body metabolism, and lipid metabolism. (F, H) Proliferation of LNCaP cells (F) and C4-2 cells (H) under regular conditions, androgen-deprivation (DHT), or steroid-deprivation (CSS) conditions, measured by optical density (OD450 nm) after transfection with siNC

or siHMGCS2. (G, I) Ketone body levels in LNCaP (G) and C4-2 (I) cells after siHMGCS2 transfection in different culture conditions. (J) Relative viability of LNCaP cells treated with sgNC, siKMT2D, or siKMT2D combined with β-hydroxybutyrate (β-OHB) rescue.

Supplementary Figure 7

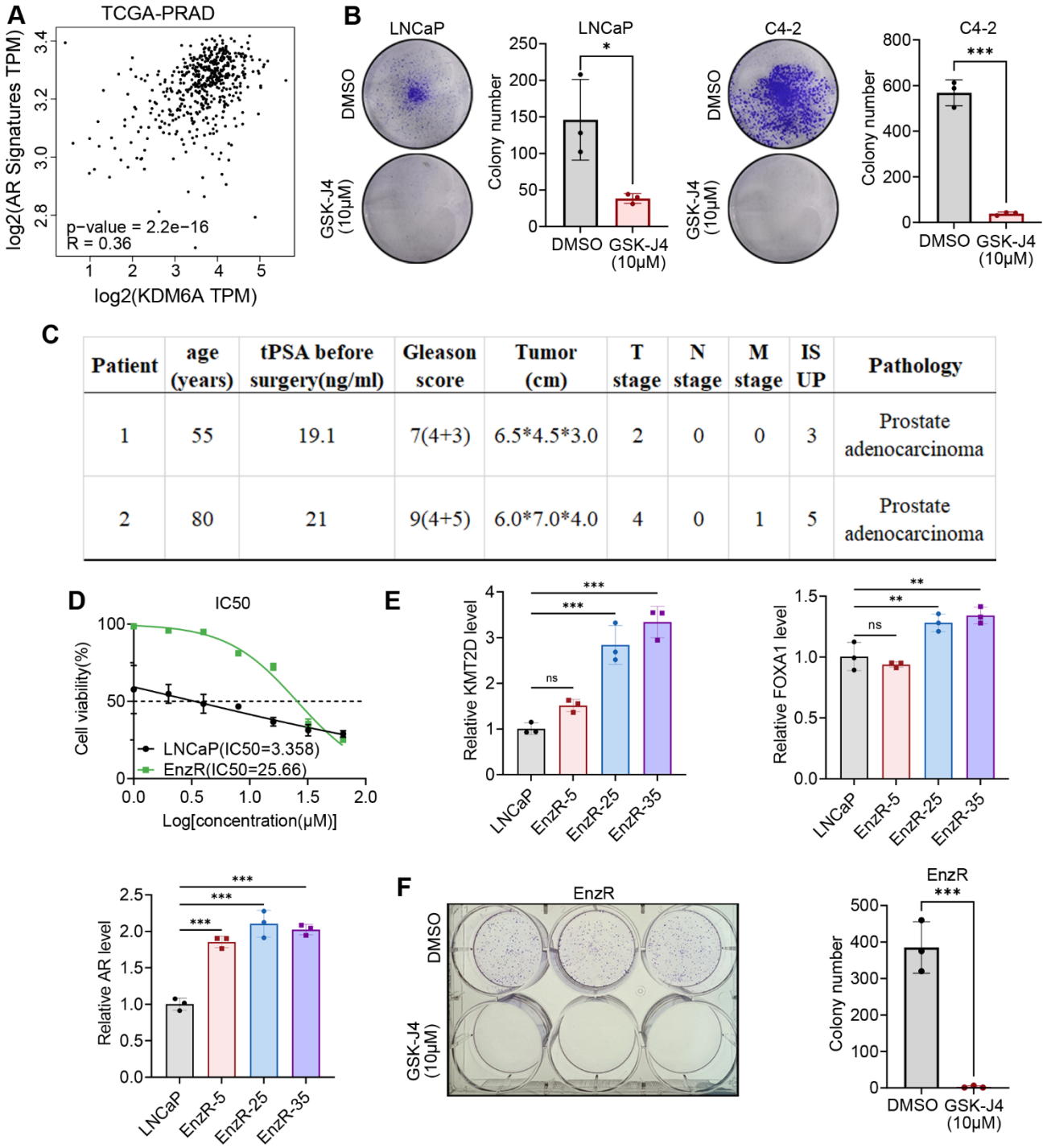

Patient	age (years)	tPSA before surgery(ng/ml)	Gleason score	Tumor (cm)	T stage	N stage	M stage	ISUP	Pathology
1	55	19.1	7(4+3)	6.5*4.5*3.0	2	0	0	3	Prostate adenocarcinoma
2	80	21	9(4+5)	6.0*7.0*4.0	4	0	1	5	Prostate adenocarcinoma

Supplementary Figure 7. Targeting KMT2D-associated H3K4me1 methylation suppresses AR signaling and overcomes enzalutamide resistance in prostate cancer. (A) Scatter plot showing positive correlation between KDM6A (UTX) expression and AR signature scores in TCGA-PRAD dataset (Pearson R = 0.36, P = 2.2e-16). (B) Representative colony formation assays and quantification for LNCaP and C4-2 cells treated with UTX inhibitor GSK-J4 (10 μM) or DMSO control, demonstrating significant growth suppression. (C) Clinical parameters of two prostate cancer patients providing tumor samples for *ex vivo* patient-derived tumor

fragment (PDTF) assays. (D) Enzalutamide dose-response curves for parental LNCaP and enzalutamide-resistant (EnzR) LNCaP cells, confirming resistance phenotype with increased IC50 in EnzR cells. (E) qRT-PCR analysis showing elevated KMT2D, FOXA1, and AR mRNA expression in EnzR sublines compared to parental LNCaP cells. (F) Colony formation assay of EnzR cells treated with GSK-J4 (10 μM) or DMSO, indicating potent inhibition of resistant cell growth.

Supplementary Table. S1 Primer list

qRT-PCR		
Gene name	Forward	Reverse
KLK3	GGAAATGACCAGGCCAAGAC	CCAGCTTCTGCTCAGTGCTT
TMPRSS2	TGCTCCAACTCTGGGATAGA	GGATGAAGTTTGGTCCGTAGAG
NKX3.1	CCATACCTGTACTGCGTGGG	TGCACTGGGGGAATGACTTA
KMT2D	CCCTTTTTGCAGTTGGGGTG	GAGGCCACGGGATTCTTCAT
FOXA1	GAAGACTCCAGCCTCCTCAACTG	TGCCTTGAAGTCCAGCTTATGC
HMGCS2	AAGTCTCTGGCTCGCCTGATGT	TCCAGGTCCTTGTTGGTGTAGG
GAPDH	CTCCTCACAGTTGCCATGTA	GTTGAGCACAGGGTACTTTATTG
β-actin	GAGAAAATCTGGCACCACACC	ATACCCCTCGTAGATGGGCAC
ChIP-qPCR and CUT&Tag-qPCR		
KLK3-enh	GCCTGGATCTGAGAGAGATATCATC	ACACCTTTTTTTTTCTGGATTGTTG
KLK2-enh	GCCTTTGCTCAGAAGACACA	ACAAGAGTGGAAGGCTCTGG
TMPRSS2-enh	TGGTCCTGGATGATAAAAAAAGTTT	GACATACGCCCCACAACAGA
NKX3.1-enh	CTGGCAAAGAGCATCTAGGG	GGCACTTCCTGAGCAAACTT
FKBP5-enh	CCCCCCTATTTTAATCGGAGTAC	TTTTGAAGAGCACAGAACACCCT
spike-in-1	ACCACTACCGCAGGAAAAGG	ACCGGATATCCCACAGGTGA
spike-in-2	GCGAGACAGCGACGAAGTAT	CCTTGTTTTCCTCGCACGAC
siRNA oligo sequence		
Gene name	sense (5 -3)	antisense (5 -3)
KMT2D-1	GCAAAUCGCUAGCAUCAUUTT	AAUGAUGCUAGCGAUUUGCTT
KMT2D-2	GCAUGAAGCCGCAGCAAUUTT	AAUUGCUGCGGCUUCAUGCTT
KMT2D-3	GAUAUUAGCUACCACACAUTT	AUGUGUGGUAGCUAAUAUCTT
KMT2D-4	GAAAGGGCACUGAGGGAUATT	UAUCCCUCAGUGCCCUUUCTT
FOXA1-1	GCGACUGGAACAGCUACUATT	UAGUAGCUGUUCCAGUCGCTT
FOXA1-2	GCGUACUACCAAGGUGUGUTT	ACACACCUUGGUAGUACGCTT
HMGCS2-1	GGUCUACUUCCCAGCCCAATT	UUGGGCUGGGAAGUAGACCTT
HMGCS2-2	GGCUCUGGUUUAGCAGCAATT	UUGCUGCUAAACCAGAGCCTT
sgKMT2D target DNA sequence		
sgKMT2D	CAGAGACCTCTCCCACATGT	
sgKMT2D PCR primer		
KMT2D-Forward	5’CATCACTCTGATCCACTCAG3’	
KMT2D-Reverse	5’GGACACACAAGCATCAGTAC3’	